

# Tri-band (L<sub>1</sub>, L<sub>2</sub>, L<sub>5</sub>) GPS Antenna with Reduced Backlobes

Yoonjae Lee<sup>(1)</sup>, Suman Ganguly<sup>(1)</sup> and Raj Mittra<sup>(2)</sup>

<sup>(1)</sup>*Center for Remote Sensing, Inc., 3702 Pender Drive, Suite 170, Fairfax, VA22033, USA*

<sup>(2)</sup>*Electromagnetic Communication Laboratory, 319 Electrical Engineering East,  
The Pennsylvania State University, University Park, PA16802, USA*

## INTRODUCTION

A GPS modernization effort [2] was announced in 1999 for the benefit of the military and civilian communities. Two navigation signals will be available for civilian use. The first signal (L<sub>2</sub>C) will be allocated in the current L<sub>2</sub> band and the second signal will be available in the new L<sub>5</sub> band. The L<sub>5</sub> signal, combined with current L<sub>1</sub> and L<sub>2</sub> signals, will provide the extended capabilities of navigation, positioning and timing services. The 24MHz bandwidth extensions for the current L<sub>1</sub> and L<sub>2</sub> signals are also proposed to carry new codes.

This paper describes a new antenna design for the recent development of the GPS technology. The new antenna covers the L<sub>5</sub> band as well as the current L<sub>1</sub> and L<sub>2</sub> bands, with enhanced performance characteristics, including increased bandwidth, very low axial ratio, superior multipath rejection, etc.

The multipath signals can be mitigated by using a low backlobe antenna. A conventional approach to mitigate the multipath interference is to use a choke ring ground plane. Choke ring ground planes consist of multiple concentric rings shorted at the bottom and open at the top. The heights of the rings are usually chosen to be a quarter-wavelength. The choke ring ground plane effectively reduces the multipath signals; however, it significantly increases the antenna size, making its adoption difficult in applications that need small form factor antennas. Alternative technologies have been pursued using the Electromagnetic Band Gap (EBG) structures [3].

We present a new structure, the “vertical choke ring”, to reduce the backlobes of the antenna. The vertical choke ring is as effective as a conventional choke ring ground plane, and yet the increase of the antenna size is kept minimal.

## ANTENNA DESIGN AND CHARACTERISTICS

Circular polarization is required for GPS applications. Circularly polarized patch antennas can be constructed using various structures and configurations such as slot-loaded patches, near-square patches, square patches with orthogonal feeding, etc. These configurations perform well for a single frequency; however, in order to achieve a multiband capability, the design must be modified, and difficulties often arise in maintaining a good circular polarization as well as a wide bandwidth at each operating band. Aperture-coupled microstrip antennas, in which the energy from feed lines is coupled to patches through apertures in the ground plane, have become very popular. Aperture-coupled configurations have advantages such as increased bandwidth, simple feed structure, and design robustness.

The vertical layout of the designed antenna is shown in Fig. 1. The antenna consists of two circular patches stacked on dielectric substrates. The two patches are excited by slots located in the ground plane. The feed line is printed on the backside of the ground plane. Circular polarization is achieved by using multiple slots on the ground plane, with proper phase delays at each slot. The top patch resonates at the upper band (L<sub>1</sub>) and the bottom patch covers the lower two bands (L<sub>2</sub> and L<sub>5</sub>). The top patch has two functionalities: to cover the L<sub>1</sub> band, and to provide a broadband characteristic with the aid of the bottom patch as a parasitic element. The slot locations and dimensions are critical for realizing good circular polarization, as well as a low return loss, at all of the operating bands.

The first step in the design procedure is to determine the dimensions of the patches. For thin substrates ( $h \ll 0.05\lambda$ ), the resonant frequency of the microstrip antenna is well approximated by the cavity model. The resonant frequencies for the TM<sub>mn0</sub><sup>z</sup> of the circular patch antenna are given by

$$(f_r)_{mn0} = \frac{1}{2\pi\sqrt{\mu\epsilon}} \left( \frac{\chi'_{mn}}{a} \right) \quad (1)$$

where  $\chi'_{mn}$  is the zeros of the derivative of the Bessel function  $J_m(x)$  and  $a$  is the radius of the circular patch. The patch radius for the dominant mode is given by [4]

$$a_e = a \left\{ 1 + \frac{2h}{\pi a \epsilon_r} \left[ \ln \left( \frac{\pi a}{2h} \right) + 1.7726 \right] \right\}^{1/2} \quad (2)$$

The antenna has been fabricated on Rogers dielectric substrates (RT/Duroid<sup>®</sup> 5880 and RO3010). The patches, slots, and microstrip feed lines are chemically etched. In order to reduce the radiation from the feeding strip line, the stacked patch element has been encapsulated in microwave absorbing materials (ECCOSORB<sup>®</sup>). The dimensions of the fabricated antenna are: diameter of approximately 204mm and height of 60mm. The return loss characteristic of the fabricated antenna has been measured using an HP-8510 network analyzer and the result is plotted in fig. 3. We note that the antenna shows good matching characteristics and broad bandwidths at all the operating bands. The antenna patterns have been measured in an anechoic chamber. Figs. 4-6 show the measured RHCP and LHCP patterns for the tri-band antenna without the vertical choke ring. The cross-polarization levels for the front side of the antenna are approximately -20dB for all the three operating bands and the back lobe levels of RHCP patterns are as low as -30dB. The Down/Up gain ratios are also plotted in Figs. 7-9. For the sake of comparison, the Pinwheel<sup>™</sup> GPS-602 [5] antenna was also measured, and its characteristics compared to those of the vertical choke ring antenna. The tri-band antenna with vertical choke ring has roll-off characteristic similar to the Pinwheel<sup>™</sup> antenna at both the L<sub>1</sub> and L<sub>2</sub> frequencies, but the back lobe levels of the tri-band antenna for 140° < theta < 180° are lower than that of the Pinwheel<sup>™</sup> antenna at both L<sub>1</sub> and L<sub>2</sub> frequencies. At the L<sub>1</sub> band, the Pinwheel<sup>™</sup> antenna shows approximately -20 dB Down/Up gain ratio up to theta=40° and approximately 0.6dB/deg roll-off after that. The tri-band GPS antenna with vertical choke ring shows better Down/Up gain ratio in the range theta<30°.

## CONCLUSIONS

A promising, patent-pending, new antenna has been presented. The designed antenna covers existing two bands as well as the new L<sub>5</sub> band. The antenna is compatible with the future system in which the bandwidth requirement is increased by 20 percent. The antenna offers good circular polarization, broad bandwidth and uniform hemispherical gain pattern for all the operating bands, and provides an excellent multipath rejection characteristic. The new structure effectively suppresses backlobes without an increase in the size of the ground plane.

## REFERENCES

- [1] Y. Lee, S. Ganguly, and R. Mittra, "Multifrequency antenna with reduced rear radiation and reception," US Patent pending (Appl. No. 10/657,824).
- [2] <http://gps.losangeles.af.mil/jpo/>.
- [3] Y. Lee, J. Yeo and R. Mittra, "Investigation of electromagnetic bandgap (EBG) structures for antenna pattern control," *IEEE Antennas and Propagation Society International Symposium*, Vol. 2, pp. 1115-1118, June, 2003.
- [4] L. C. Shen, S. A. Long, M. R. Allerding, and M. D. Walton, "Resonant Frequency of a Circular Disk, Printed-Circuit Antenna," *IEEE Trans. Antennas Propagat.*, Vol. AP-25, No.4, pp.595-596, July 1977.
- [5] W. Kunysz, "High Performance GPS Pinwheel antenna," [http://www.novatel.com/Documents/Papers/gps\\_pinwheel\\_ant.pdf](http://www.novatel.com/Documents/Papers/gps_pinwheel_ant.pdf).

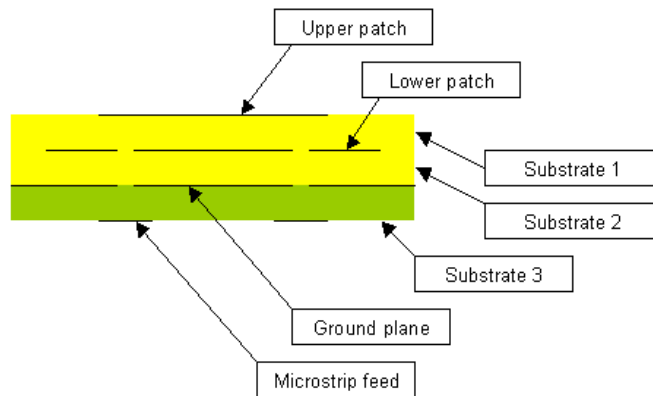


**Fig. 1.** Vertical profile of the antenna element

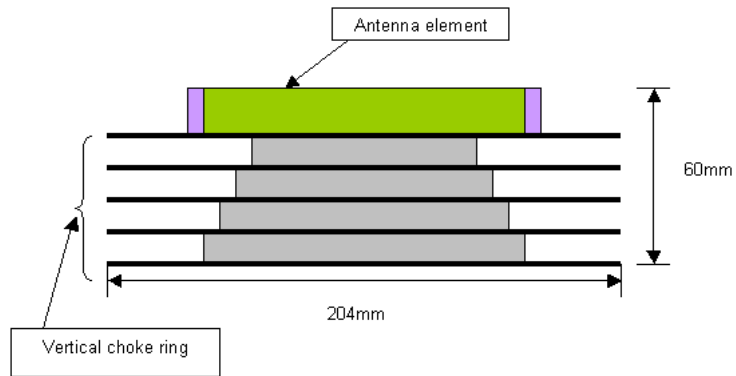


**Fig. 2.** Antenna geometry

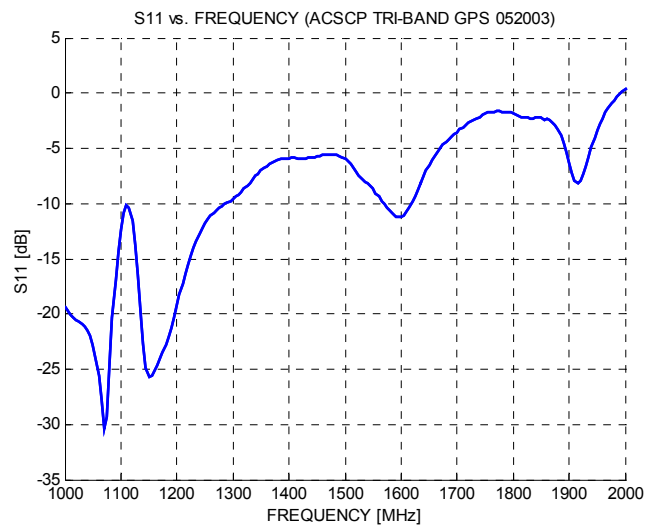


**Fig. 3.** Measured  $S_{11}$  characteristic

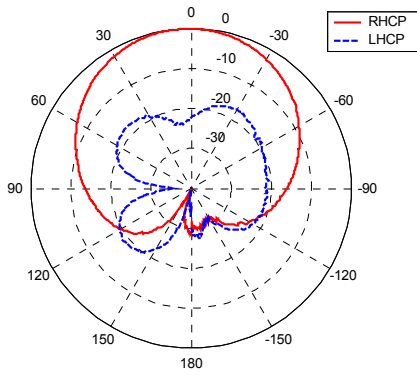


**Fig. 4.** Measured antenna pattern (L<sub>1</sub>)

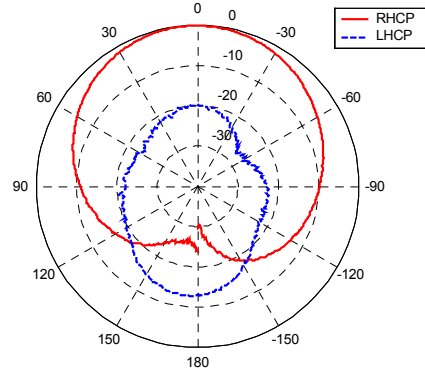


**Fig. 5.** Measured antenna pattern (L<sub>2</sub>)

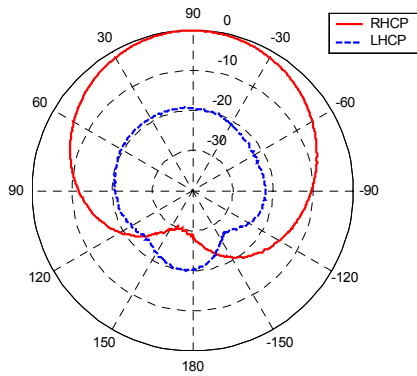


**Fig. 6.** Measured antenna pattern (L<sub>5</sub>)

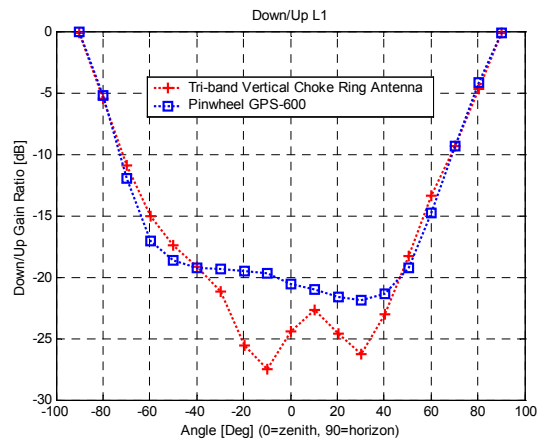


**Fig. 7.** Measured Down/Up ratio gain (L<sub>1</sub>)

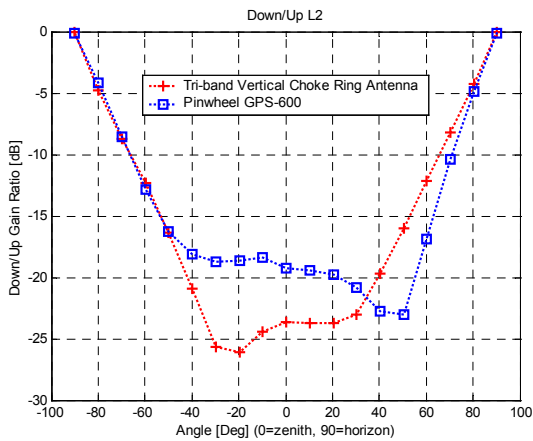


**Fig. 8.** Measured Down/Up ratio gain (L<sub>2</sub>)

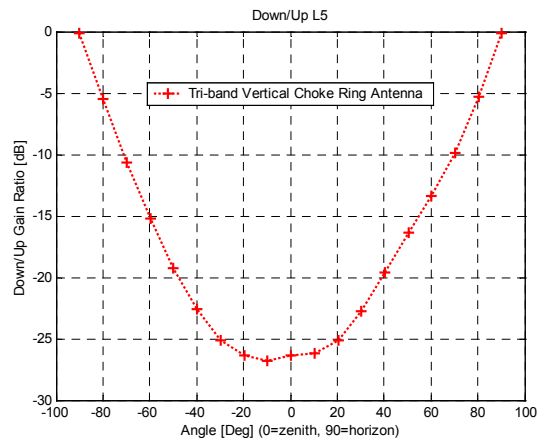


**Fig. 9.** Measured Down/Up ratio gain (L<sub>5</sub>)